2014 IEEE International Conference on Robotics & Automation (ICRA)
Hong Kong Convention and Exhibition Center
May 31 - June 7, 2014. Hong Kong, China

A System for Automated Counting of Fetal and Maternal Red Blood Cells in Clinical KB Test

J. Ge[1], Z. Gong[1], J. Chen[1], J. Liu[1], J. Nguyen[1], Z.Y. Yang[1], C. Wang[2], and Y. Sun[1]

***Abstract*— The Kleihauer-Betke test (KBT) is a widely used method for measuring fetal-maternal hemorrhage (FMH) in maternal care. In hospitals, KBT is performed by a certified technologist to count a minimum of 2,000 fetal and maternal red blood cells (RBCs) on a blood smear. Manual counting is inherently inconsistent and subjective. This paper presents a system for automated counting and distinguishing fetal and maternal RBCs on clinical KB slides. A custom-adapted hardware platform is used for KB slide scanning and image capturing. Spatial-color pixel classification with spectral clustering is proposed to separate overlapping cells. Optimal clustering number and total cell number are obtained through maximizing cluster validity index. To accurately identify fetal RBCs from maternal RBCs, multiple features including cell size, shape, gradient and saturation difference are used in supervised learning to generate feature vectors, to tackle cell color, shape and contrast variations across clinical KB slides. The results show that the automated system is capable of completing the counting of over 60,000 cells (vs. 2,000 by technologists) within 5 minutes (vs. 15 minutes by technologists). The counting results are highly accurate and correlate strongly with those from benchmarking flow cytometry measurement.**

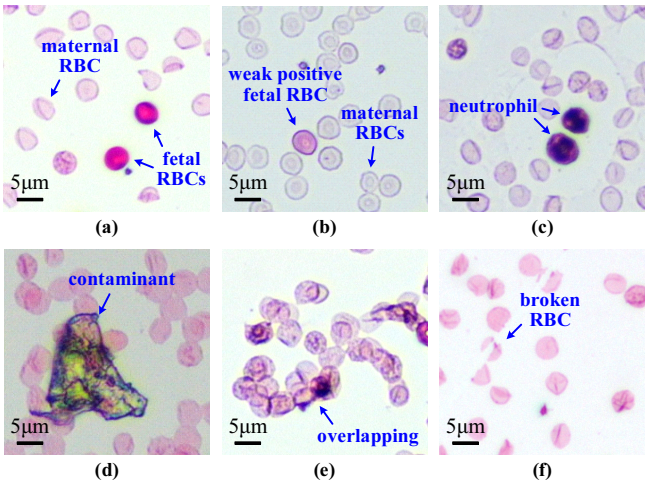

Fig. 1. Sample images from clinical KB slides. (a) 'canonical' fetal and maternal RBCs; (b) weak positive fetal RBC; (c) neutrophils; (d) contaminant; (e)(f) severally overlapping and broken RBCs.

I. Introduction

In North America, there are over 6 million pregnancies annually. Rhesus D hemolytic disease of the newborn (RhD HDN) is a serious alloimmune condition, where fetal red blood cells (RBCs) are destroyed by the maternal immune system through the placenta. During pregnancy or child birth, the mother may be exposed to the infant's blood, and this causes the development of antibodies (IgG) against the Rhesus antigen, which can destruct the Rh positive fetal RBCs by passing through the placenta into the fetus and lead to hemolysis [1]. Fetal-maternal hemorrhage (FMH) can have devastating consequences for fetus, such as anemia, hydrops, neurologic injury, erythroblastosis, stillbirth, and neonatal death. Hence, quantification of FMH is necessary for physicians to make treatment decisions, for instance, the administration of an appropriate therapeutic dose of RhD immune globulin (RhIG) [2].

Besides Rh diseases, FMH can also result from the loss of integrity of the normal physiological barrier between the fetal and maternal circulation, which must be quantified in pregnancy care for prompt treatment (e.g., blood transfusion) [3]. The standard clinical method of quantitating FMH is the KB test [4]. The test takes advantage of the differential resistance of fetal and maternal hemoglobin to acid (fetal hemoglobin is significantly more resistant). A standard blood smear is prepared from the mother's blood (1:1,000 dilution with PBS). After drying, staining and incubating, the blood smear slides are counted under a microscope by certified personnel. Since the fetal hemoglobin is resistant to the citrate buffer, the resulting bright-pink cells are classified as fetal cells [see Fig. 1(a)]. The percentage of FMH can then be calculated [5].

In present clinical practice, fetal RBCs and total number of RBCs are manually estimated by certified technologists who look into the eyepieces of a microscope and count a minimum of 2,000 cells. Inherently, manual KB test is subjective and inconsistent, which can often result in underestimation/overestimation of fetal RBC count and wide variations across technologists and hospitals [6].

Flow cytometry is an accepted benchmark technique for counting fetal and maternal RBCs, based on the fetal hemoglobin-specific antibody. The flow cytometric analysis of FMH involves multiple pre-treatment steps, which requires more than 30 minutes pre-process and has high personnel-skill requirements [7]. Due to these limitations, flow cytometry testing is typically unavailable during after hours in hospitals. The infrastructure cost along with operating and reagent costs also limits the clinical routine use of flow cytometry for KB tests [8]. The adoption of flow cytometry for fetal/maternal RBC counting has been discussed for two decades in transfusion medicine [9]; however, the state-of-the-art practice in most hospitals for quantifying FMH is still

[1]The authors are with Dept. of Mechanical and Industrial Engineering, University of Toronto, 5 King's College Road, Toronto, ON M5S 3G8, Canada sun@mie.utoronto.ca

[2]Chen Wang is with Mount Sinai Hospital, 600 University Ave., Toronto, ON M5G 1X5 Canada cwang@mtsinai.on.ca

manual KB test that relies on manual counting of fetal and maternal RBCs.

Fig.1(a) shows canonical fetal and maternal RBCs that can be easily counted and distinguished. However, many KB slides have more complex patterns that make the tasks difficult. As shown in Fig.1(b)-(f), KB slide preparation (inherent difference in blood samples and staining unevenness) often results in cell overlapping; the presence of random contaminants; variations in cell color, size and shape; contrast variations between cells and slide background across KB slides. Fetal RBC identification is also made challenging due to the existence of neutrophils and weak positive fetal RBCs. Automated RBC counting requires the segmentation of overlapping cells and the identification of fetal RBCs to be properly and reliably handled. A few attempts were made to automate fetal and maternal RBC counting [6], [10], where automation in these works refers to the use of commercial motorized stage to capture cell images. Fetal RBCs were distinguished from maternal RBCs based on intensity and distribution patterns of staining by a technologist. The total cell number on a KB slide was also manually estimated. No system exists that is capable of automated counting of total RBC numbers and fetal RBCs.

A number of image segmentation methods have been reported for cell counting. Non-maximum suppression and seeded region growing were applied to segment corneal epithelial cells [4]. A critical issue in automated cell counting is to effectively segment overlapping cells. Major approaches for separating overlapping cells include watershed [11], template matching [12], and color-texture based segmentation [13]. Due to the existence of regional maxima, the watershed algorithm often leads to over segmentation. Template matching has low efficiency and requires large quantities of cell samples to achieve reasonable accuracy. Overlapping cells with close colors or textures can be clustered by color-texture based segmentation [13]; however, they cannot be separated from each other for quantification.

Due to the complex characteristics of RBCs on clinical KB slides, spectral clustering with spatial-color information is proposed in this paper to segment overlapping cells. Each cell can be considered a cluster since the color within a cell is relatively homogeneous. Besides color values, spatial information of each cell is also added to construct features used for generating similarity matrices. Cluster validity index is then used for determining the number of clusters.

To distinguish fetal RBCs from maternal RBCs, color information is the foremost cue. Due to variations in cell color, size, and the overlapping extent across KB slides, relying solely on saturation channel information is unreliable. Hence, supervised clustering method is used in our system for fetal RBC identification, where feature vector is constructed with cell color, size, shape, gradient, saturation difference between a cell and the whole slide.

II. System Design

As shown in Fig. 2, the system consists of a standard optical microscope, the manual stage of which was motorized

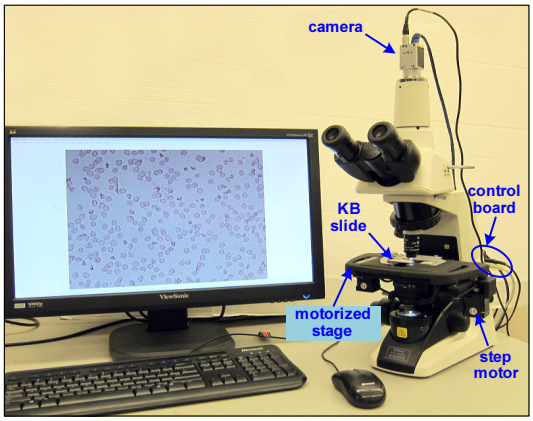

Fig. 2. System for automated image capturing and counting of fetal and maternal RBCs on clinical KB slides.

with timing belts, pulleys, and stepping motors. The motorized stage has a positioning accuracy of $\pm 19\mu$m and $\pm 26\mu$m along the X and Y directions. The resolution is comparable for each direction and is $20\pm 3\mu$m. Travel distances for positioning a KB slide are 10mm and 35mm along X and Y, respectively. Due to the non-uniform distribution of RBCs on a KB slide, which is more severe on the far left and far right parts of the slide, images should be captured around the slide center. Hence, two motion limit switches along the X and Y directions are added for automatic slide centering. Under a $20\times$ objective, the system typically captures 120 images around the slide center (image size: 2560×1920) for automated counting.

FMH quantification and RhIG drug dose calculation rely on accurately determining the percentage of fetal RBCs. The number of vials (300 μg/vial) of RhIG administered to patients is calculated as [14]

$$N_{vial} = \frac{2370 \cdot \sqrt{h \cdot w/3131} \cdot N_{Fetal}}{30 \cdot N_{Total}} + 1 \qquad (1)$$

where h and w are the height and weight of the patient. N_{Fetal} and N_{Total} denote the fetal RBC number and total RBC number among the RBCs counted on the KB slide, which must be accurately counted.

III. Total RBC Counting

Fig. 1(e) shows an example of cell overlapping that must be reliably handled to achieve accurate counting of the total number of RBCs. To begin with, a target needs to be determined to be an isolated cell or overlap with other cells. For this purpose, we use the concavity points searching method [15]. If a cell is isolated without any concavity points, the cell is counted as one cell directly. Otherwise, segmentation as discussed below is conducted.

In overlapping RBCs, each cell forms a cluster due to the similar color within the same cell. Hence, segmenting overlapping cells can be considered cluster analysis. Among existing clustering methods, the k-means algorithm is effective only for clusters with similar sizes and densities, a condition that is not true in overlapping RBCs on a KB

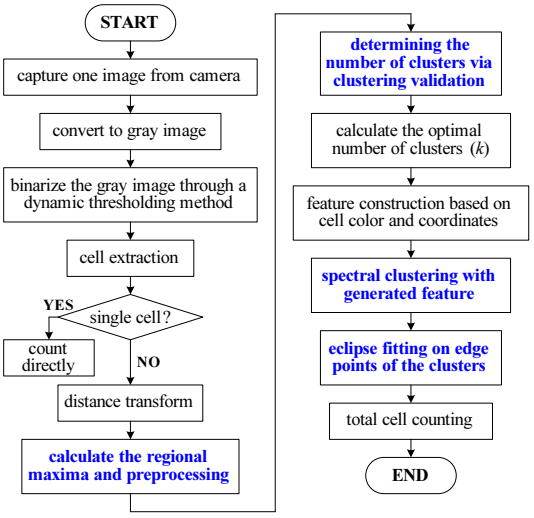

Fig. 3. Flow chart of total RBC counting.

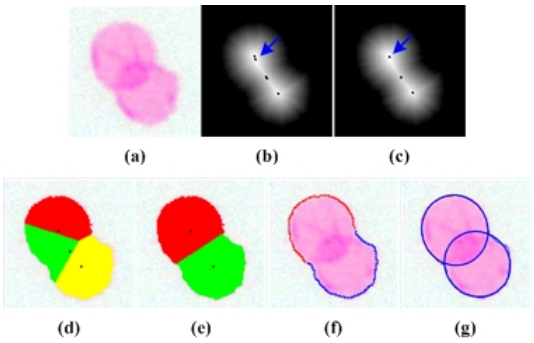

Fig. 4. Cluster number determination. (a) Original image; (b) regional maxima (blue arrow labeled); (c) spurious maxima eliminated; (d) spectral clustering result with k=3, SV_3 = 0.1652; (e) spectral clustering result with k=2, SV_2 = 0.6173; (f) edge points with two clusters; (g) ellipse fitting.

slide. Furthermore, the k-means algorithm is sensitive to initial centers and usually converges to a local optimum. In comparison, the spectral clustering algorithm (SC) [16] is capable of recognizing clusters with unusual shapes and obtaining global optimal solutions with eigen-decomposition. Unfortunately, only depending on cell color, the SC algorithm can mistakenly group those pixels belonging to different RBCs although they locate far from each other in the image.

Hence, in our system, spatial information (i.e., pixel coordinates) besides color is used to generate feature vectors used for calculating the similarity matrix of SC. This spatial and color-based spectral clustering approach is proven in our work effective in separating overlapping RBCs. Fig. 3 shows the sequence of processing for counting the total number of RBCs on a KB slide. Key steps are highlighted in blue and described in the following sub-sections.

A. Regional Maxima Preprocessing

We observed that many extracted regional maxima in a distance image are located closely (Fig. 4(b)). If overlapping cells are segmented directly with the number of regional maxima, over segmentation often occurs. Thus, we defined a distance-dependent rule to eliminate those spurious maxima.

repeat
  $\forall m = (x_m, y_m) \in S$
  if $\exists n = \{(x_n, y_n) | D(m,n) \leqslant D_{TH})\}$ **then**
    select $p = \{m, n | max(x_m, x_n)\}$
    update S
  end if
until no changes in S

where m and n are regional maxima within maxima set S; D is the Euclidean distance between two arbitrary maxima; D_{TH} is the minimal distance threshold. Considering that the radius of typical RBCs is approximately 20 pixels under a 20× microscope objective, D_{TH} in our system is set to 10. If the Euclidean distance $D(m, n)$ between point m and n is smaller than 10, the point with larger coordinate in the x direction is selected into the set S (see Line 3 and Line 4 of the rule). Fig. 4(c) shows that spurious maxima are removed after regional maxima preprocessing.

B. Determination of Optimal Number of Clusters

In cluster analysis of overlapping cells, the initial number of clusters is obtained through counting the number of local maxima after regional maxima preprocessing, and then cluster validation is applied to determine the number of overlapping cells. Cluster validity index SV [17], consisting of two evaluation criteria of the cells (i.e., separation S and compactness V), is

$$SV(k,V,X) = \frac{S_k}{V_k} = \frac{\sum_{i=1}^{k} \min\limits_{j\in[1,\ldots,k], i\neq j} d(v_i, v_j)}{\sum_{i=1}^{k} \max\limits_{x_j \in C_i} d(x_j, v_i)} \qquad (2)$$

where $X = \{x_j; j = 1,2,\cdots,n\}$ denotes the dataset with n data points. Dataset X then can be partitioned into k clusters C_i and each cluster has a centroid v_i, here $i = 1,2,\cdots,k$. Separation measure S_k is the sum of pairwise minimal inter-cluster distances in a k-cluster structure while compactness measure V_k indicates how different the members of each cluster are. The smaller of value V_k is, the compacter of the clusters are. The optimal cell number is obtained through maximizing the SV index.

As an example shown in Fig. 4(d)(e), SV_2=0.6173 is larger than SV_3=0.1652, indicating that the result of segmentation is more appropriate with two clusters. In Fig. 4(e), after determining the optimal number of clusters and generating features based on cell color and spatial coordinates, the system applies spectral clustering to classify the overlapping cells (labeled red and green). Subsequently, contours in the overlapped areas are predicted via ellipse fitting [18] (Fig. 4(g)) since most RBCs on a KB slide have circle-like or ellipse-like shapes.

IV. Fetal RBC Identification

In manual KB test, fetal RBC identification is conducted through human visual inspection relying on cell patterns such

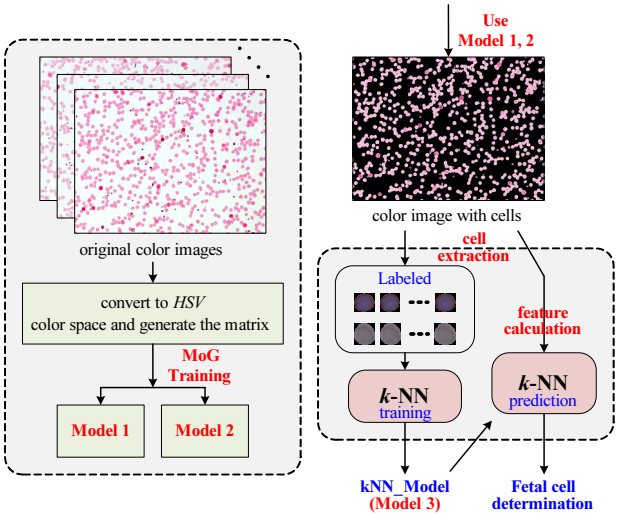

Fig. 5. Flowchart of supervised learning for identifying fetal RBCs.

as color, size, shape, and texture [6]. However, feature variations across KB slides exist although hospital technologists closely follow slide preparation protocols. In our system, supervised learning is used, and the process is illustrated in Fig. 5.

As shown in Fig. 5, all the 120 raw color images are read into the memory and converted to the hue, saturation, value (HSV) color space. An $N\times3$ dimensional matrix X_1 constructed with all image pixels' H, S, and V values is fit with a two-component Gaussian mixture distribution. Here, N equals to $2560\times1920\times120$, and Model 1 is generated for separating all RBC pixels from background pixels. In the converted color space, fetal and maternal RBCs show significant differences in the saturation channel. Therefore, combining saturation values of the cells singled out by Model 1 forms $N_{Scell}\times1$ matrix X_2. Model 2 is generated for separating fetal RBCs from maternal RBCs, fit with another two-component Gaussian mixture distribution.

In captured color images, fetal RBCs appear red-colored, brilliant, shining, and smooth inside while maternal ones appear light and pinkish. Therefore, color information is used to identify fetal cells. Due to cell variations across KB slides, besides color information, our system also integrates other features, such as cell size, roundness, gradient, saturation difference between a cell and the whole slide, to distinguish fetal RBCs from maternal ones. Based on these features, the system applies a non-parametric learning algorithm (k-nearest neighbor, kNN) via supervised learning to improve RBC classification accuracy. The kNN method is suitable for this purpose since it is not certain whether the generated feature vectors of the fetal or maternal RBCs will satisfy such assumptions as Gaussian mixtures and linear separation. Additionally, the kNN method does not generalize the many training vectors and makes decisions based on the entire training feature vectors.

In this paper, more than 3,500 cells (labeled "positive" or "negative") were calculated for generating feature vectors.

$$Feature = (H_i, S_i, V_i, R_i, G_i, B_i, Gd_i, D_i) \tag{3}$$

where i = 1,2,$\cdots$,3500; H, S, V, R, G, and B denote six channel values in HSV and RGB color space; Gd is the gradient of the cell; D is the saturation difference between cell and whole slide.

A kNN model (Model 3) is built after fitting the feature vector with the kNN algorithm. Features of extracted cells are calculated and predicted with Model 3 where similarity of RBCs is calculated and verified according to

$$\begin{cases} \varsigma_{FC}^{i} = 1, & p_i > Th_f \\ \varsigma_{FC}^{i} = 0, & others \end{cases} \tag{4}$$

where ς_{FC}^{i} denotes the fetal RBC indicator of ith cell. p_i represents similarity between ith cell and labeled "positive" cells. Th_f denotes the fetal RBC threshold value. Typically, this threshold value is set to 0.5 according to statistical characteristics gathered from more than 50 clinical KB slides. Therefore, fetal RBC number is determined by $\sum_{i=1}^{N}\varsigma_{FC}^{i}$, where N is the total cell number in the 120 images.

V. Experimental Results and Discussion

A. Total RBC Counting

Fig. 6 shows overlapping cells randomly selected from KB slides. Comparisons between marker-controlled watershed [11], color and texture based segmentation algorithm [13], k-means clustering algorithm, and our proposed spatial-color-based spectral clustering approach are made.

Column (a) to (c) show slightly overlapping situations where almost all the algorithms segmented cells reasonably well, except that over segmentation occurred in (2, a) due to the wrong markers that existed within the overlapping area (arrow labeled). For the more severally overlapping situations (see column (d) to (f)), marker-controlled watershed in row 2 yielded over segmentation due to many spurious maxima that appeared in the overlapping areas. k-means clustering in row 4 divided the overlapping cells into several regions; however, it led to erroneous segmentations due to the incorrect initial centers and number of clusters.

Most cell pixels were extracted with the color and texture clustering method, as shown in (3, a), (3, b) and (3, e). Unfortunately, only some scattered pixels or contours were picked out in other three columns in row 3, due to color and texture unevenness of the RBCs. This algorithm can extract the cells out but is not effective in separating them from each other. Our proposed algorithm (spatial-color-based spectral clustering) generates a new feature vector by adding spatial information into the original color matrix, which is proven effective in segmenting overlapping cells (see row 5 in Fig. 6). Furthermore, contour fitting on the overlapping cells generates clear ellipse-like contours for cell quantification.

Fig. 7 shows the segmentation and counting results of one KB image. The overlapping cells were segmented, and their contours were labeled with black ellipses. Those isolated cells, labeled with blue plus symbols, were counted directly without segmentation procedures. To evaluate the accuracy

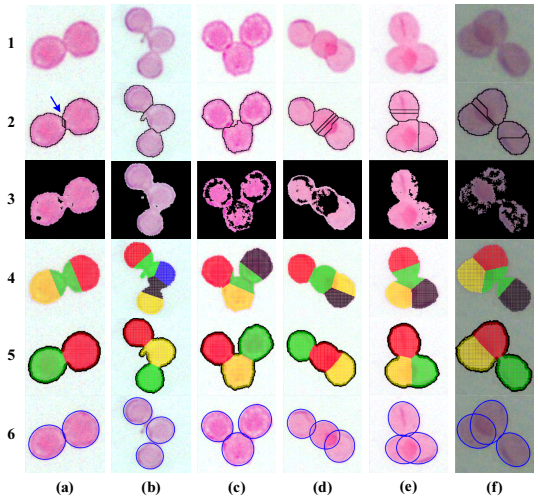

Fig. 6. Segmentation results using different algorithms. (1) original image; (2) marker-controlled watershed [11]; (3) color and texture based segmentation [13]; (4) k-means algorithm; (5)(6) our proposed spatial-color based spectral clustering; and ellipse fitting on cell contours.

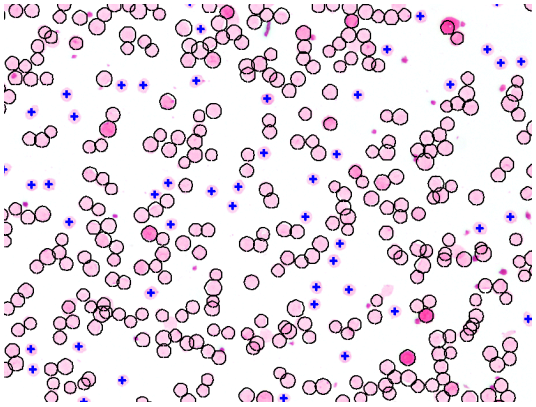

Fig. 7. Automated total RBC counting. Isolated RBCs are labeled with blue plus. Overlapping cells are segmented and fit with black eclipses.

of total RBC counting, 8 KB images were randomly selected and counted with the marker-controlled watershed method, our proposed spatial-color spectral clustering algorithm, and manual counting. Manual counting was conducted by a skilled technologist who used computer mouse clicking to count every cell in the images and then spent significant time carefully verifying every single cell. The manual counting results were used to calculate over-counting and under-counting rates summarized in Table I.

The marker-controlled watershed algorithm resulted in much higher over-counting ratios, ranging from 13% to 20%, due to its nature in severe over segmentation. Our proposed algorithm performed significantly better in terms of both over-counting and under-counting rates. Scrutinizing the segmentation results using our spatial-color spectral clustering approach, we observed that some under-counted cells were missed because of their significantly lower contrasts compared to surrounding cells. There were only 3 to 6 cells over-counted, and verification revealed they were cells broken into more than one segment, as illustrated in Fig. 1(f).

TABLE I

TOTAL CELL COUNTING (UC: UNDERCOUNTED; OC: OVERCOUNTED)

Img	technologist	marker-controlled watershed			proposed algorithm		
	#total	#UC/ratio	#OC/ratio	#total	#UC/ratio	#OC/ratio	#total
1	584	15 /2.27%	92 / 13.9%	661	6 / 1.03%	4 / 0.69%	582
2	669	12 / 1.57%	105 / 13.8%	762	9 / 1.35%	6 / 0.90%	666
3	531	10 / 1.67%	79 / 13.2%	600	3 / 0.56%	3 / 0.56%	531
4	543	8 / 1.28%	88 / 14.1%	623	5 / 0.92%	3 / 0.55%	541
5	611	17 / 2.37%	122 / 17.0%	716	5 / 0.82%	1 / 0.16%	607
6	624	15 / 2.11%	101 / 14.2%	710	7 / 1.13%	4 / 0.64%	621
7	643	20 / 2.57%	156 / 20.0%	779	10 / 1.57%	4 / 0.63%	637
8	653	18 / 2.32%	141 / 18.2%	776	8 / 1.23%	3 / 0.46%	648

TABLE II

COUNTING RESULTS: AUTOMATED COUNTING; MANUAL COUNTING BY TECHNOLOGIST

Group	Slide	Automated			Technologist	Known
		#Fetal	#Total	Ratio		
1	1	89	79273	0.11%	0.09%	0.1%
	2	73	86144	0.09%	0.13%	
	3	95	103216	0.09%	0.11%	
2	1	389	82669	0.47%	0.52%	0.5%
	2	442	86584	0.51%	0.55%	
	3	400	81649	0.49%	0.49%	
3	1	702	75675	0.93%	0.89%	1%
	2	749	77148	0.97%	0.91%	
	3	811	80261	1.01%	1.05%	

B. Fetal RBC Counting and Blind KB Tests

To quantify the accuracy of fetal cell identification using supervised learning, nine slides (three per group) with known fetal cell concentrations (0.1%, 0.5% and 1%) were tested. These 'artificial' KB slides were prepared through accurately controlled mixing of fetal blood from umbilical cord and adult RBCs. Results from automated counting and hospital technologist reading are summarized in Table II.

Data in Table II is graphically shown in Fig. 8. Our automated system determined on the nine 'artificial' KB slides average fetal RBC concentrations to be 0.097%, 0.49% and 0.97% with standard deviations of 0.012%, 0.02%, and 0.04%. The results from technologist reading were 0.11%, 0.52% and 0.95% with standard deviations of 0.02%, 0.03%, and 0.09%. Compared to the known mixing ratios on these 'artificial' KB slides, the results quantitatively confirmed the automated system's capability for highly accurate RBC counting. Note that our automated system counted over 60,000 cells per KB slide while standard technologist reading was limited to 2,000 cells. Additionally, automated counting is completed within 5 minutes per slide while manual reading costs ∼15 minutes.

Another 44 KB slides were made from pregnant patient samples collected in the Mount Sinai Hospital were

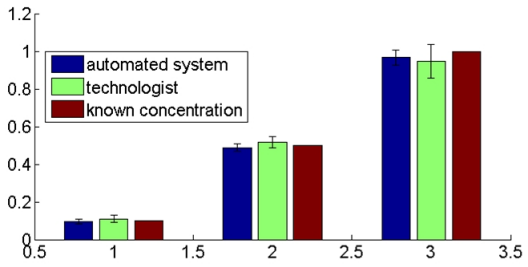

Fig. 8. Comparison between technologist reading and automated counting.

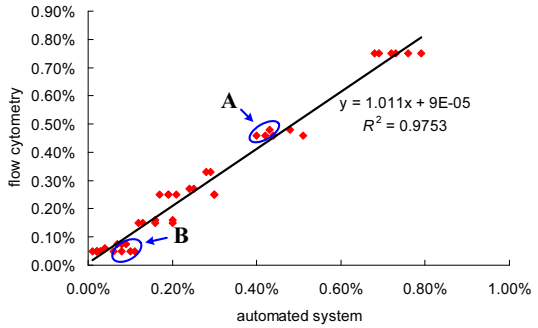

Fig. 9. Correlation between automated counting and flow cytometry in 44 pregnant patient samples (R^2=0.9753).

tested. Testing results using our automated system strongly correlated with those from benchmarking flow cytometry measurement (R^2=0.9753 shown in Fig. 9 vs. R^2=0.9436 between technologist reading and flow cytometry, data not shown). Counting accuracy is defined as

$$Accuracy = \frac{TP+TN}{TP+TN+FP+FN} \tag{5}$$

where TP is the number of true positives, FP is the number of false positives, TN is the number of true negatives and FN is the number of false negatives. The counting accuracy of our automated system was quantified to be 0.984±0.09 (vs. 0.926±0.15 in technologist reading).

C. Discussion

The data points labeled 'A' in Fig. 9 are those fetal concentrations determined by the automated system to be lower than flow cytometry. We re-evaluated those slides and observed that colors of some fetal RBCs appeared much lighter compared to 'canonical' fetal RBCs shown in Fig. 1(a). These lighter fetal RBCs were considered by the automated system negative. For those slides (labeled 'B') with higher fetal RBC concentrations than determined by flow cytometry, some negative RBCs appeared darker and brighter than surrounding cells, leading to higher false positives. Our next step is to include more patient samples and larger training datasets to further improve the automated system's accuracy and correlation with flow cytometry.

VI. Conclusion

This paper described an automated system for fetal and maternal RBC reading in clinical KB test. The system uses a custom-motorized image capturing platform to automatically center a KB slide, collect ∼120 images (over 60,000 cells), and count/distinguish fetal and maternal RBCs. Spatial-color classification with spectral clustering is proposed to effectively count overlapping cells. Multiple features including cell color, size, shape and contrast variations are used in supervised learning for distinguishing fetal RBCs and maternal ones. Testing patient KB slides, the automated system quantitatively demonstrated high accuracy in counting and strong correlation with benchmarking flow cytometry. Compared to manual technologist reading, the automated system is significantly more efficient and accurate.

References

[1] J. M. Bowman, B. Chown, M. Lewis, and J. M. Pollock, "Rh isoimmunization during pregnancy: antenatal prophylaxis." *Canadian Medical Association journal*, vol. 118, no. 6, pp. 623–7, Mar. 1978.

[2] C. Chen, S. Cheng, C. Lee, F. Chang, C. Wu, and Y. Yuh, "Fetomaternal Hemorrhage," *Journal of Medical Science*, vol. 23, no. 4, pp. 231–234, 2003.

[3] Z. Wang, J. Shi, Y. Zhou, and C. Ruan, "Detection of red blood cell-bound immunoglobulin G by flow cytometry and its application in the diagnosis of autoimmune hemolytic anemia." *International journal of hematology*, vol. 73, no. 2, pp. 188–93, Feb. 2001.

[4] N. Bandekar, A. Wong, D. Clausi, and M. Gorbet, "A novel approach to automated cell counting for studying human corneal epithelial cells." in *International Conference of the IEEE EMBS*, Boston, Jan. 2011, pp. 5997–6000.

[5] W. C. Warger II, J. A. Newmark, B. Zhao, C. M. Warner, and C. A. DiMarzio, "Accurate cell counts in live mouse embryos using optical quadrature and differential interference contrast microscopy," in *Pro. of SPIE*, J.-A. Conchello, C. J. Cogswell, and T. Wilson, Eds., Feb. 2006, pp. 609 009–12.

[6] D. M. Pelikan, S. a. Scherjon, W. E. Mesker, G. M. de Groot-Swings, G. G. Brouwer-Mandema, H. J. Tanke, and H. H. Kanhai, "Quantification of fetomaternal hemorrhage: a comparative study of the manual and automated microscopic Kleihauer-Betke tests and flow cytometry in clinical samples." *American journal of obstetrics and gynecology*, vol. 191, no. 2, pp. 551–7, Aug. 2004.

[7] D. Huh, W. Gu, Y. Kamotani, J. B. Grotberg, and S. Takayama, "Microfluidics for flow cytometric analysis of cells and particles." *Physiological measurement*, vol. 26, no. 3, pp. R73–98, June 2005.

[8] Y. Mundee, N. C. Bigelow, B. H. Davis, and J. B. Porter, "Simplified flow cytometric method for fetal hemoglobin containing red blood cells." *Cytometry*, vol. 42, no. 6, pp. 389–93, Dec. 2000.

[9] J. D. Hoyer, C. S. Penz, V. F. Fairbanks, C. a. Hanson, and J. a. Katzmann, "Flow cytometric measurement of hemoglobin F in RBCs: diagnostic usefulness in the distinction of hereditary persistence of fetal hemoglobin (HPFH) and hemoglobin S-hPFH from other conditions with elevated levels of hemoglobin F." *American journal of clinical pathology*, vol. 117, no. 6, pp. 857–63, June 2002.

[10] D. M. V. Pelikan, W. E. Mesker, S. a. Scherjon, H. H. H. Kanhai, and H. J. Tanke, "Improvement of the Kleihauer-Betke test by automated detection of fetal erythrocytes in maternal blood." *Cytometry. Part B, Clinical cytometry*, vol. 54, no. 1, pp. 1–9, July 2003.

[11] R. Rodríguez, T. E. Alarcón, and O. Pacheco, "A new strategy to obtain robust markers for blood vessels segmentation by using the watersheds method." *Computers in biology and medicine*, vol. 35, no. 8, pp. 665–86, Oct. 2005.

[12] C. Chen, W. Wang, J. A. Ozolek, and G. K. Rohde, "A flexible and robust approach for segmenting cell nuclei from 2D microscopy images using supervised learning and template matching." *Cytometry. Part A*, vol. 83, no. 5, pp. 495–507, May 2013.

[13] M. Datar, D. Padfield, and H. Cline, "Color and texture based segmentation of molecular pathology images using HSOMS," in *2008 5th IEEE International Symposium on Biomedical Imaging: From Nano to Macro*. IEEE, May 2008, pp. 292–295.

[14] G. Ramsey, "Inaccurate doses of Rh immune globulin after Rh-incompatible fetomaternal hemorrhage: survey of laboratory practice." *Archives of pathology & laboratory medicine*, vol. 133, no. 3, pp. 465–9, Mar. 2009.

[15] M. Farhan, O. Yli-Harja, and A. Niemistö, "An improved clump splitting method for convex objects," in *Proceedings of the 7th Workshop on Computational Systems Biology*, 2010, pp. 35–38.

[16] J. Shi and J. Malik, "Normalized cuts and image segmentation," *IEEE Transactions on Pattern Analysis and Machine Intelligence*, vol. 22, no. 8, pp. 888–905, 2000.

[17] K. R. Zalik and B. Zalik, "Validity index for clusters of different sizes and densities," *Pattern Recognition Letters*, vol. 32, no. 2, pp. 221–234, Jan. 2011.

[18] A. Fitzgibbon, M. Pilu, and R. Fisher, "Direct least square fitting of ellipses," *IEEE Transactions on Pattern Analysis and Machine Intelligence*, vol. 21, no. 5, pp. 476–480, May 1999.